High-Pressure Behavior of Solid H_2, D_2, He^3, He^4, and Ne^{20} †

E. L. Pollock, T. A. Bruce, G. V. Chester, and J. A. Krumhansl
Laboratory of Atomic and Solid State Physics, Cornell University, Ithaca, New York 14850
(Received 24 May 1971)

The failure of the harmonic approximation for the lattice dynamics of solid H_2, D_2, He^3, and He^4 at densities corresponding to pressures below the order of 10^3 atm is well known. We present evidence that the equation of state for solid H_2, D_2, He^3, He^4, and Ne^{20} at high densities may, however, be calculated successfully in the harmonic approximation. Equation-of-state curves at high density for H_2, D_2, He^3, He^4, and Ne^{20} (all for the fcc phase at $T=0$ °K) are given and compare well with results from Monte Carlo or cluster-expansion treatments using a Jastrow wave function. The comparison with experiment shows good agreement in the high-density range for He^3, He^4, and Ne^{20}. For D_2 and H_2 the theoretical results agree closely with each other at high densities, but not so well with the experimental data of Stewart in that region, suggesting inadequacy either of the potential or of the experimental data. For the Lennard-Jones and Buckingham potentials used for pressures ranging from a few thousand to several million bars the Domb-Salter approximation gives an accurate result for the zero-point energy of the harmonic crystal. Our results lead us to conclude that for good high-density computations the necessary short range correlations are adequately accounted for in the harmonic approximation.

I. INTRODUCTION

The lattice dynamics of solid H_2, D_2, He^3, and He^4 at densities corresponding to low pressures must be treated by the methods applicable to quantum crystals. In particular, the harmonic approximation (HA) predicts instability for all four crystals at densities corresponding to pressures below the order of 10^3 bar. We shall present evidence however that for higher densities the harmonic approximation works with increasing accuracy.

It is also shown that, for the potentials used and over the density range examined, the Domb-Salter approximation[1] gives an accurate result for the zero-point energy of the harmonic crystal. For fcc H_2 at $T=0$ °K, results obtained in this approximation are compared with two other calculations based on methods suitable for quantum crystals: a Monte Carlo computation using a Jastrow wave function[2] and a truncated-cluster-expansion treatment of a similar wave function by the method of L. H. Nosanow,[3] with the important difference that different Jastrow functions[3,4] from Nosanow gave computational convergence over a wide density range. A Lennard-Jones 6-12 and a Buckingham exp-6 potential are used for H_2. For fcc He^3, He^4, and Ne^{20} at $T=0$ °K, the Lennard-Jones potential is used and compared with Monte Carlo results.

In addition to the substantial agreement in the energy and pressure at high density calculated by these various methods, the decreasing ratio of kinetic to total energy at increasing density and a similar decrease for the ratio of rms particle displacement to nearest-neighbor distance indicate the validity of the harmonic approximation at high densities.

II. ZERO-POINT ENERGY AND PARTICLE DISPLACEMENT AT $T=0$ IN THE HA

In the HA the Helmhotz free energy for the lattice is[5]

$$F = V_0 + \frac{1}{2}\sum_{k,j}\hbar\omega_j(k) + \frac{1}{\beta}\sum_{k,j}\ln(1-e^{-\beta\hbar\omega_j(k)}) \quad , \tag{2.1}$$

where V_0 is the potential energy for the rigid lattice. At $T=0$ this reduces to

$$E = V_0 + \frac{1}{2}\sum_{k,j}\hbar\omega_j(k) = V_0 + \tfrac{3}{2}N\hbar\langle\omega^1\rangle \quad , \tag{2.2}$$

with

$$\langle\omega^r\rangle \equiv \frac{1}{3N}\sum_{k_j}\omega_j^r(k) \tag{2.3}$$

for a lattice of N particles. We will be interested specifically only in the fcc lattice. For the potentials used here V_0 is obtainable from published tables[6] or by simple computation.

The second term, or zero-point energy, can be calculated by expressing the first moment $\langle\omega\rangle$ in terms of the even moments of the lattice vibration spectrum. As shown below (2.14) the even moments are obtained from the trace of various powers of the dynamical matrix. For a given potential the even moments may be evaluated numerically by a method due to Isenberg.[7] In fact this scheme will be used at only a few densities to show that the simpler Domb-Salter approximation (explained below) gives accurate results for the zero-point energy (although the full scheme can be used routinely with slightly more effort).

From the identity

$$\omega_j(k) = \omega_0[\,1 - \omega_j'(k)^2/\omega_0^2]^{1/2} \quad , \tag{2.4}$$

where

$$\omega_j'(k)^2 = \omega_0^2 - \omega_j^2(k) \quad , \tag{2.5}$$

we have

$$\omega_j(k) = \omega_0 \sum_{r=0}^{\infty} (-1)^r \binom{\frac{1}{2}}{r} \left(\frac{\omega_j'(k)}{\omega_0}\right)^{2r} \quad . \tag{2.6}$$

With the notation

$$J(n) = \frac{1}{3N} \sum_{kj} [\omega_j'(k)]^n \quad , \tag{2.7}$$

$$\langle \omega \rangle = \frac{1}{3N} \sum_{kj} \omega_j(k) = \omega_0 \sum_{r=0}^{\infty} (-1)^r \binom{\frac{1}{2}}{r} \frac{J(2r)}{\omega_0^{2r}} \quad . \tag{2.8}$$

The $J(2r)$ can be written in terms of the even moments using (2.7) with (2.5). The parameter ω_0 is to be chosen for rapid convergence.

The $\omega_j^2(k)$ are, of course, eigenfrequencies of the dynamical matrix D:

$$\omega_j^2(k) \vec{e}\binom{k}{j} = \overleftrightarrow{D}(k) \vec{e}\binom{k}{j} \quad , \quad j = 1,2,3; \quad k = 1, \ldots, N \tag{2.9}$$

$$D_{\alpha\beta}(k) = \sum_l \frac{\Phi_{\alpha\beta}(l)}{M} e^{-i\vec{k}\cdot\vec{x}_l} \quad , \tag{2.10}$$

$$\Phi_{\alpha\beta}(|\,l - l'\,|) = \Phi_{\alpha\beta}(ll') = \frac{\partial^2 V}{\partial u_\alpha(l)\, \partial u_\beta(l')} \quad . \tag{2.11}$$

The total potential energy of the lattice is V and $u_\alpha(l)$ denotes the particle displacements from equilibrium. From the completeness relation

$$\sum_j e_\alpha\binom{k}{j} e_\beta^*\binom{k}{j} = \delta_{\alpha\beta} \quad , \tag{2.12}$$

and (2.9) the second moment may be expressed as

$$3N\langle \omega^2 \rangle = \sum_k \mathrm{Tr}\, \overleftrightarrow{D}(k) \quad . \tag{2.13}$$

Multiplying (2.9) by the dynamical matrix the required number of times and using the completeness relation gives the general expression

$$3N\langle \omega^{2r} \rangle = \sum_k \mathrm{Tr}\, \overleftrightarrow{D}^r(k) \quad . \tag{2.14}$$

From this equation and the definition of the dynamical matrix (2.10) the even moments may also be expressed in terms of the force constants. In particular, for the second moment

$$\langle \omega^2 \rangle = (1/3M) \sum_\alpha \Phi_{\alpha\alpha}(0) \quad . \tag{2.15}$$

Starting with the expression[8]

$$\langle u^2(l) \rangle = \sum_\alpha \langle u_\alpha^2(l) \rangle = \frac{\hbar}{2NM} \sum_{kj} \frac{\coth \frac{1}{2}\beta\hbar\omega_j(k)}{\omega_j(k)} \quad , \tag{2.16}$$

$$\langle u^2(l) \rangle \to \frac{\hbar}{2NM} \sum_{kj} \frac{1}{\omega_j(k)} \text{ as } T \to 0 \quad . \tag{2.17}$$

At $T = 0$ the square displacement is related to the inverse first moment. In the same way as for the first moment we may write

$$\frac{1}{\omega_j(k)} = \frac{1}{\omega_0} \left(1 - \frac{\omega_j'(k)^2}{\omega_0^2}\right)^{-1/2} \quad , \tag{2.18}$$

$$\frac{1}{\omega_j(k)} = \frac{1}{\omega_0} \sum_r (-1)^r \binom{-\frac{1}{2}}{r} \left(\frac{\omega_j'(k)}{\omega_0}\right)^{2r} \quad , \tag{2.19}$$

so

$$\langle \omega^{-1} \rangle = \frac{1}{\omega_0} \sum_r (-1)^r \binom{-\frac{1}{2}}{r} \frac{J(2r)}{\omega_0^{2r}} \tag{2.20}$$

and

$$\langle u^2(l) \rangle = \frac{3\hbar}{2M\omega_0} \sum_r (-1)^r \binom{-\frac{1}{2}}{r} \frac{J(2r)}{\omega_0^{2r}} \quad . \tag{2.21}$$

III. DOMB AND SALTER APPROXIMATION

In the case of a Debye spectrum the spectrum moments are given by the relation

$$\langle \omega^r \rangle = 3\omega_D^r/(3+r) \quad . \tag{3.1}$$

Using this expression, the zero-point energy per particle for the Debye crystal is

$$\frac{E_{\text{zero}}}{N} = \tfrac{3}{2}\hbar\langle \omega \rangle = \tfrac{9}{8}\hbar\omega_D \quad . \tag{3.2}$$

Domb and Salter suggest as a better approximation to the zero-point energy replacing ω_D in (3.2) by $\omega_D(\infty)$ as determined from the relation

$$\omega_D^2(\infty) = \tfrac{5}{3}\langle \omega^2 \rangle \tag{3.3}$$

and $\langle \omega^2 \rangle$ is determined exactly from (2.15). With $\omega_0 = \omega_D(\infty)$ in the exact relation (2.8), the zero-point energy may be written

$$\frac{E_{\text{zero}}}{N} = \tfrac{3}{2}\hbar\omega_D(\infty) \sum_r (-1)^r \binom{\frac{1}{2}}{r} \frac{J(2r)}{\omega_D^{2r}(\infty)} \quad . \tag{3.4}$$

If the Domb-Salter approximation were exact, we would have

$$\sum_r (-1)^r \binom{\frac{1}{2}}{r} \frac{J(2r)}{\omega^{2r}(\infty)} = \frac{3}{4} \quad . \tag{3.5}$$

This sum is hereafter referred to as the Domb-Salter factor. Similarly we might hope to approximate the relation

$$\langle \omega^{-1} \rangle = \tfrac{3}{2}\omega_D^{-1} \tag{3.6}$$

derived from the Debye spectrum by

$$\langle \omega^{-1} \rangle = \tfrac{3}{2}\omega_D^{-1}(\infty) \quad . \tag{3.7}$$

From (2.20) this is true if

$$\sum_r (-1)^r \binom{-\frac{1}{2}}{r} \frac{J(2r)}{\omega_D^{2r}(\infty)} = \frac{3}{2} \quad . \tag{3.8}$$

This sum will be called the squared displacement factor.

The first seven even moments for an fcc lattice with interactions between three nearest-neighbor

TABLE I. Domb-Salter and displacement factors. The sums representing these factors were truncated after the seventh even moment. Examination of the size of successive terms indicates that this truncation may cause an error of roughly ± 0.002 for the Domb-Salter factor and ± 0.02 for the displacement factor. The moments involved were evaluated with the assumption of interactions with three nearest-neighbor shells.

Lennard-Jones potential Domb-Salter factor	Displacement factor	$\rho\left(\frac{\text{particles}}{\sigma^3}\right)$	$\rho\left(\frac{\text{mole}}{\text{cm}^3}\right)_{He}$	$V\left(\frac{\text{cm}^3}{\text{mole}}\right)_{He}$	$\rho\left(\frac{\text{mole}}{\text{cm}^3}\right)_{H_2}$	$V\left(\frac{\text{cm}^3}{\text{mole}}\right)_{H_2}$
0.740	1.47	11.66	1.16	0.86	0.748	1.34
0.740	1.47	5.49	0.545	1.84	0.352	2.85
0.740	1.47	4.0	0.398	2.51	0.257	3.90
0.740	1.47	3.0	0.299	3.35	0.193	5.19
0.741	1.47	2.31	0.229	4.37	0.148	6.76
0.741	1.46	1.82	0.181	5.52	0.117	8.56
0.742	1.46	1.46	0.145	6.90	0.094	10.7
0.744	1.45	1.185	0.118	8.49	0.076	13.15
0.748	1.43	0.98	0.097	10.3	0.063	15.9

shells were evaluated at several different densities by the method of Isenberg for the Lennard-Jones and Buckingham potentials used. Using these moments in (3.5) and (3.8), the accuracy of these approximations is shown (Tables I–VI).

IV. POTENTIALS AND FORCE CONSTANTS

The potentials used here are the Lennard-Jones 6-12 potential

$$V(r)=4\epsilon\left[(\sigma/r)^{12}-(\sigma/r)^{6}\right] \quad , \tag{4.1}$$

with $\epsilon=36.7$ °K and $\sigma=2.958$ Å for[9] H_2, and $\epsilon=10.22$ °K and $\sigma=2.556$ Å for He^3 and He^4.[10] For H_2 the calculations were repeated with the Buckingham exp-6 potential

$$V(r)=\begin{cases}\dfrac{\epsilon}{1-6/\alpha}\left[\dfrac{6}{\alpha}\exp\alpha\left(1-\dfrac{r}{r_m}\right)-\left(\dfrac{r_m}{r}\right)^6\right] , & r>r_{\max}\\ \infty , & r<r_{\max}\end{cases} \tag{4.2}$$

where[11]

$$\alpha=14.9, \qquad r_m=3.339 \text{ Å},$$

$$\epsilon=38.02 \text{ °K} , \quad r_{\max}=0.7864 \text{ Å} .$$

The force constants for a crystal characterized by these potentials are easily derived. For the Lennard-Jones case

$$\Phi_{\substack{\alpha\beta\\ l\neq 0}}(l)=-\frac{24\epsilon}{\sigma^2}\left[x_\alpha(l)x_\beta(l)\left(\frac{28}{r_l^{16}}-\frac{8}{r_l^{10}}\right)-\delta_{\alpha\beta}\left(\frac{2}{r_l^{14}}-\frac{1}{r_l^{8}}\right)\right], \tag{4.3}$$

where all distances are in units of σ,

$$\Phi_{\alpha\beta}(0)=-\sum_{l\neq 0}\Phi_{\alpha\beta}(l) \ . \tag{4.4}$$

Since the sums in $\Phi_{\alpha\alpha}(0)$ are tabulated for the Lennard-Jones potential and may be used in (2.15) to determine $\langle\omega^2\rangle$, this allows a partial check to be made on the computations of the even moments by the Isenberg method. For the Buckingham potential

$$\Phi_{\substack{\beta\gamma\\ l\neq 0}}(l)=\frac{\epsilon}{(1-6/\alpha)r_m^2}\left\{\frac{6}{r_l}\exp\alpha(1-r_l)\times\left[\delta_{\beta\gamma}-\frac{x_\beta(l)\,x_0(l)}{r_l}\left(\frac{1}{r_l}+\alpha\right)\right]+\frac{1}{r_l^8}\left(\frac{8x_\beta(l)x_0(l)}{r_l^2}\right)\right\}-\delta_{\beta\gamma} , \tag{4.5}$$

where all distances in units of r_m; the nearest-neighbor distance is substantially larger than $r_{\max}$ at all densities considered.

V. EQUATION OF STATE IN DOMB-SALTER APPROXIMATION

The data in Table I shows that the Domb-Salter approximation for the zero-point energy holds over

TABLE II. For the density range shown the maximum error in using the Domb-Salter approximation is less than 1.5% for the Lennard-Jones potential and less than 3.5% for the Buckingham potential. The results for the Lennard-Jones apply for any crystal with the density in units of particles $/\sigma^3$ since the potential strength and particle mass enter as a scaling factor for the frequencies [see Eq. (4.3)] and cancel from Eq. (3.5) and (3.8). The same is not true for the Buckingham potential since the parameter α also appears.

Domb-Salter factor	Displacement factor	ρ(mole/cm^3)
0.725	1.54	0.748
0.733	1.51	0.324
0.739	1.48	0.134
0.743	1.46	0.081
0.754	1.40	0.053

the density range considered with an error of less than 3.5% for both potentials. We shall calculate the equation of state using this approximation as it allows a simple form in the case of both potentials.

For the Lennard-Jones potential

$$P(\epsilon, \Lambda, V) = \frac{\epsilon}{V}\left(4(2S^{12} - S^6) + (\tfrac{3}{2})^{1/2}\Lambda \frac{(77S^{14} - 10S^8)}{(4.4S^{14} - S^8)^{1/2}}\right), \quad (5.1)$$

where V is the volume per particle (or molecule for H_2). The deBoer parameter

$$\Lambda = \hbar/(M\epsilon)^{1/2} \quad (5.2)$$

and

$$S^n = \sum_l (1/r_l^n) \quad (r \text{ in units of } \sigma) . \quad (5.3)$$

For the fcc lattice

$$S^6 = 14.453\,921\,1/d^6 , \quad S^8 = 12.801\,937\,2/d^8 ,$$
$$S^{12} = 12.131\,880\,2/d^{12} , \quad S^{14} = 12.058\,992\,0/d^{14} .$$

The nearest-neighbor distance d is in σ units. The form (5.1) follows easily from using Domb-Salter approximation for the zero-point energy [(3.2) and (3.3)] with the second moment determined from (2.15) and (4.4). Differentiating with respect to the volume gives (5.1).

With the Buckingham potential

$$P = \frac{\epsilon_0}{V}\left(\frac{5}{8}\frac{\hbar}{(M\epsilon_0)^{1/2}r_m}\frac{\exp\alpha(\alpha^2 S^3 - 2S^1 - 2\alpha S^2) - 40S^8}{[\frac{10}{3}(\exp\alpha(\alpha S^2 - 2S^1) - 5S^8)]^{1/2}} + \exp\alpha S^3 - S^6\right) . \quad (5.4)$$

All distances in (5.4) and (5.5) are in units of r_m and $\epsilon_0 = \epsilon/(1 - 6/\alpha)$,

$$S^n = \sum_l r_l^{n-2} e^{-\alpha r_l} , \quad n = 1, 2, 3 . \quad (5.5)$$

VI. DISCUSSION

The energy and pressure calculated in the Domb-Salter approximation (for an fcc crystal with masses and potential parameters appropriate to

TABLE III. Domb-Salter approximation for H_2 (Lennard-Jones potential). ρ is the density and d is the nearest-neighbor distance.

ρ (mole/cm^3)	d (Å)	Zero-point energy (°K)	Static potential energy (°K)	Total energy (°K)	Pressure (bar)
0.2023	0.2266E 01	0.4234E 04	0.1657E 05	0.2080E 05	0.1459E 07
0.1902	0.2313E 01	0.3651E 04	0.1239E 05	0.1604E 05	0.1066E 07
0.1789	0.2360E 01	0.3156E 04	0.9245E 04	0.1240E 04	0.7837E 06
0.1686	0.2408E 01	0.2735E 04	0.6876E 04	0.9611E 04	0.5791E 06
0.1590	0.2455E 01	0.2376E 04	0.5086E 04	0.7462E 04	0.4300E 06
0.1502	0.2502E 01	0.2068E 04	0.3731E 04	0.5799E 04	0.3208E 06
0.1420	0.2550E 01	0.1803E 04	0.2795E 04	0.4508E 04	0.2403E 06
0.1344	0.2597E 01	0.1575E 04	0.1927E 04	0.3502E 04	0.1808E 06
0.1273	0.2644E 01	0.1378E 04	0.1338E 04	0.2716E 04	0.1364E 06
0.1207	0.2692E 01	0.1208E 04	0.8931E 03	0.2101E 04	0.1033E 06
0.1145	0.2739E 01	0.1059E 04	0.5575E 03	0.1617E 04	0.7848E 05
0.1088	0.2786E 01	0.9305E 03	0.3056E 03	0.1236E 04	0.5976E 05
0.1034	0.2834E 01	0.8181E 03	0.1178E 03	0.9358E 03	0.4560E 05
0.0984	0.2881E 01	0.7198E 03	−0.2102E 02	0.6987E 03	0.3485E 05
0.0937	0.2928E 01	0.6336E 03	−0.1222E 03	0.5113E 03	0.2667E 05
0.0893	0.2976E 01	0.5578E 03	−0.1947E 03	0.3631E 03	0.2043E 05
0.0852	0.3023E 01	0.4912E 03	−0.2452E 03	0.2459E 03	0.1565E 05
0.0813	0.3070E 01	0.4323E 03	−0.2790E 03	0.1533E 03	0.1198E 05
0.0777	0.3118E 01	0.3803E 03	−0.3001E 03	0.8018E 02	0.9168E 05
0.0742	0.3165E 01	0.3341E 03	−0.3116E 03	0.2255E 02	0.7003E 04
0.0710	0.3212E 01	0.2931E 03	−0.3158E 03	−0.2276E 02	0.5338E 04
0.0679	0.3260E 01	0.2565E 03	−0.3148E 03	−0.5828E 02	0.4056E 04
0.0651	0.3307E 01	0.2237E 03	−0.3098E 03	−0.8602E 02	0.3072E 04
0.0624	0.3354E 01	0.1944E 03	−0.3020E 03	−0.1076E 03	0.2319E 04
0.0598	0.3402E 01	0.1679E 03	−0.2922E 03	−0.1244E 03	0.1747E 04
0.0574	0.3449E 01	0.1438E 03	−0.2812E 03	−0.1373E 03	0.1318E 04
0.0551	0.3496E 01	0.1219E 03	−0.2693E 03	−0.1474E 03	0.1004E 04
0.0529	0.3544E 01	0.1016E 03	−0.2570E 03	−0.1554E 03	0.7876E 03
0.0508	0.3591E 01	0.8247E 02	−0.2445E 03	−0.1621E 03	0.6621E 03
0.0489	0.3638E 01	0.6397E 02	−0.2321E 03	−0.1681E 03	0.6424E 03
0.0470	0.3686E 01	0.4490E 02	−0.2199E 03	−0.1750E 03	0.8170E 03
0.0452	0.3733E 01	0.2096E 02	−0.2081E 03	−0.1871E 03	0.2062E 04

H_2, He^3, and He^4) are compared with results of Monte Carlo calculations using a trial Jastrow wave function and with available experimental data. For H_2 comparison is made with a cluster-expansion treatment.

For a Jastrow wave function of the form

$$\psi = \prod_{i<j} f(r_{ij}) \prod_i \phi(r_i) \ , \qquad (6.1)$$

$$f(r) = e^{-(1/2)(B/r)^5} \ , \quad \phi(\vec{r}_i) = e^{-(1/2)A(\vec{r}_i - \vec{R}_i)^2} \ ,$$

where the R_i $(i = 1, \ldots, N)$ are the lattice sites and A and B variational parameters, configurational averages of the type,

$$\left\langle \frac{1}{r^n} \right\rangle_{AB\rho} = \frac{1}{N} \sum_i \sum_j \left\langle \frac{1}{r_{ij}^n} \right\rangle \ , \qquad (6.2)$$

where the expectation value is computed with (6.1) for particular values of A and B at a density ρ, may be scaled to different densities.[4] If

$$S = (\rho'/\rho)^{1/3} \ ,$$

$$A' = AS^2 \ ,$$

$$B' = B/S \ ,$$

then $\langle 1/r^n \rangle_{A'B'\rho'} = S^n \langle 1/r^n \rangle_{AB\rho}$. Since the energy computed with (6.1) is determined by $\langle 1/r^6 \rangle$, $\langle 1/r^7 \rangle$, and $\langle 1/r^{12} \rangle$ for a Lennard-Jones potential this result is sufficient for scaling the energy to new $A'B'\rho'$. In this way the energy minimum at a new density may be searched for among the $(A'B')$ values without recomputing the configurational averages (6.2).

TABLE IV. Domb-Salter approximation for H_2 (Buckingham potential). ρ is the density and d is the nearest neighbor distance.

ρ (mole/cm^3)	d (Å)	Zero-point energy (°K)	Static potential energy (°K)	Total energy °K)	Pressure (bar)
0.290	0.2007E 01	0.4342E 04	0.3677E 05	0.4111E 05	0.2855E 07
0.271	0.2054E 01	0.3941E 04	0.2962E 05	0.3356E 05	0.2229E 07
0.253	0.2101E 01	0.3576E 04	0.2380E 05	0.2738E 05	0.1741E 07
0.237	0.2148E 01	0.3244E 04	0.1909E 05	0.2233E 05	0.1066E 07
0.222	0.2196E 01	0.2941E 04	0.1526E 05	0.1820E 05	0.1066E 07
0.208	0.2243E 01	0.2666E 04	0.1216E 05	0.1482E 05	0.8352E 06
0.195	0.2290E 01	0.2416E 04	0.9648E 04	0.1206E 05	0.6549E 06
0.184	0.2337E 01	0.2188E 04	0.7619E 04	0.9807E 04	0.5139E 06
0.173	0.2384E 01	0.1981E 04	0.5982 E 04	0.7963E 04	0.4035E 06
0.163	0.2432E 01	0.1793E 04	0.4663E 04	0.6457E 04	0.3170E 06
0.154	0.2479E 01	0.1622E 04	0.3603E 04	0.5226E 04	0.2492E 06
0.146	0.2526E 01	0.1467E 04	0.2753E 04	0.4220E 04	0.1959E 06
0.138	0.2573E 01	0.1326E 04	0.2074E 04	0.3399E 04	0.1514E 06
0.130	0.2621E 01	0.1198E 04	0.1532E 04	0.2729E 04	0.1213E 06
0.124	0.2668E 01	0.1081E 04	0.1102E 04	0.2183E 04	0.9544E 05
0.117	0.2715E 01	0.9754E 93	0.7619E 93	0.1737E 04	0.7511E 05
0.111	0.2762E 01	0.8794E 03	0.4948E 03	0.1374E 04	0.5911E 05
0.106	0.2809E 01	0.7922E 03	0.2864E 03	0.1079E 04	0.4651E 05
0.101	0.2857E 01	0.7130E 03	0.1250E 03	0.8381E 03	0.3658E 05
0.096	0.2904E 01	0.6411E 03	0.1427E 01	0.6426E 03	0.2875E 05
0.091	0.2951E 01	0.5758E 03	−0.9196E 02	0.4839E 03	0.2259E 05
0.087	0.2998E 01	0.5165E 03	−0.1613E 03	0.3552E 03	0.1772E 05
0.083	0.3045E 01	0.4626E 03	−0.2115E 03	0.2510E 03	0.1389E 05
0.079	0.3093E 01	0.4136E 03	−0.2467E 03	0.1669E 03	0.1087E 05
0.076	0.3140E 01	0.3690E 03	−0.2700E 03	0.9903E 02	0.8497E 04
0.072	0.3187E 01	0.3285E 03	−0.2840E 03	0.4444E 02	0.6627E 04
0.069	0.3234E 01	0.2916E 03	−0.2909E 03	0.6292E 00	0.5157E 04
0.066	0.3282E 01	0.2579E 03	−0.2923E 03	−0.3443E 02	0.4003E 04
0.064	0.3329E 01	0.2272E 03	−0.2896E 03	−0.6243E 02	0.3102E 04
0.061	0.3376E 01	0.1991E 03	−0.2838E 03	−0.8473E 02	0.2400E 04
0.059	0.3423E 01	0.1733E 03	−0.2757E 03	−0.1025E 03	0.1858E 04
0.056	0.3470E 01	0.1495E 03	−0.2661E 03	−0.1166E 03	0.1445E 04
0.054	0.3518E 01	0.1274E 03	−0.2554E 03	−0.1280E 03	0.1140E 04
0.052	0.3565E 01	0.1068E 03	−0.2441E 30	−0.1374E 03	0.9240E 03
0.050	0.3612E 01	0.8712E 02	−0.2325E 03	−0.1454E 03	0.8004E 03
0.048	0.3659E 01	0.6789E 02	−0.2208E 03	−0.1529E 03	0.7783E 03
0.046	0.3707E 01	0.4794E 02	−0.2091E 02	−0.1612E 03	0.9568E 03
0.044	0.3754E 01	0.2288E 02	−0.1978E 03	−0.1749E 03	0.2187E 04

This technique was used to find minimum energies for He^3 and He^4 using configurational averages computed for H_2 (Ref. 2). The configurational averages used for scaling were computed by the Monte Carlo technique with relatively short runs (less than 400 moves per particle for a 108-particle system) and the mesh of A, B values available for scaling were not of a uniform density in the A-B plane, thus making location of the energy minimum sometimes slightly imprecise. The agreement between the energy determined in the Domb-Salter approximation and by Monte Carlo is nonetheless close for all three crystals (Figs. 1–3). The energy differences between the Monte Carlo and Domb-Salter energy curves for all three crystals can be seen to be much smaller than the zero-point energy, showing that the agreement is not solely due to the dominance of the static potential-energy contribution to the total energy at large densities.

As shown in Fig. 4, both the Monte Carlo calculations and the Domb-Salter approximation show a rapidly decreasing ratio of kinetic to total energy as the density increases. Numerically, the two calculations differ on this ratio. It is not possible to regard this discrepancy as significant. The kinetic energy is not a stationary quantity with respect to the variational parameters in an approximate wave function and values of A and B giving similar values for the total energy may give varying ratios of kinetic to total energy. Also a trial wave function such as (6.1) may give accurate results for the total energy while the kinetic and potential energy separately are considerably in error. Although the exact cause of the discrepancy at higher densities shown in Fig. 4 is not clear, it seemed worth presenting for completeness.

The ratio of rms displacement to nearest-neighbor distance (Fig. 5) was determined from (2.21) for six densities using the first seven even moments of the vibrational spectrum, although as mentioned earlier a Domb-Salter-type approximation allows an explicit form for this ratio as a function of nearest-neighbor distance to be written.

TABLE V. Domb-Salter approximation for He^3 (Lennard-Jones potential).

V Molar volume (ml)	Nearest-neighbor distance (Å)	Zero-point energy (°K)	Static potential energy (°K)	Total (°K)	Pressure (bar)
3.196	0.1958E 01	0.2114E 04	0.4614E 04	0.6728E 04	0.6877E 06
3.401	0.1999E 01	0.1823E 04	0.3450E 04	0.5273E 04	0.5074E 06
3.614	0.2040E 01	0.1576E 04	0.2574E 04	0.4151E 04	0.3768E 06
3.835	0.2081E 01	0.1366E 04	0.1915E 04	0.3281E 04	0.2815E 06
4.066	0.2121E 01	0.1186E 04	0.1416E 04	0.2603E 04	0.2116E 06
4.306	0.2162E 01	0.1032E 04	0.1039E 04	0.2071E 04	0.1599E 06
4.555	0.2203E 01	0.9003E 03	0.7533E 03	0.1654E 04	0.1215E 06
4.813	0.2244E 01	0.7865E 03	0.5367E 03	0.1323E 04	0.9280E 05
5.081	0.2285E 01	0.6881E 03	0.3727E 03	0.1061E 04	0.7122E 05
5.359	0.2326E 01	0.6030E 03	0.2487E 03	0.8517E 03	0.5492E 05
5.646	0.2367E 01	0.5290E 03	0.1552E 03	0.6843E 03	0.4254E 05
5.944	0.2408E 01	0.4646E 03	0.8510E 02	0.5497E 03	0.3309E 05
6.252	0.2449E 01	0.4085E 03	0.3279E 02	0.4413E 03	0.2584E 05
6.571	0.2490E 01	0.3594E 03	−0.5855E 01	0.3535E 03	0.2026E 05
6.900	0.2530E 01	0.3164E 03	−0.3404E 02	0.2823E 03	0.1594E 05
7.240	0.2571E 01	0.2785E 03	−0.5422E 02	0.2243E 03	0.1259E 05
7.591	0.2612E 01	0.2452E 03	−0.6829E 02	0.1770E 03	0.9979E 04
7.953	0.2653E 01	0.2159E 03	−0.7770E 02	0.1382E 03	0.7934E 04
8.327	0.2694E 01	0.1899E 03	−0.8356E 02	0.1063E 03	0.6330E 04
8.712	0.2735E 01	0.1668E 03	−0.8676E 02	0.8007E 02	0.5067E 04
9.108	0.2776E 01	0.1463E 03	−0.8795E 02	0.5839E 02	0.4070E 04
9.517	0.2817E 01	0.1281E 03	−0.8765E 02	0.4042E 02	0.3283E 04
9.937	0.2858E 01	0.1117E 03	−0.8626E 02	0.2546E 02	0.2660E 04
10.370	0.2899E 01	0.9705E 02	−0.8409E 02	0.1296E 02	0.2167E 04
10.815	0.2939E 01	0.8382E 02	−0.8138E 02	0.2444E 01	0.1780E 04
11.273	0.2980E 01	0.7182E 02	−0.7830E 02	−0.6476E 01	0.1477E 04
11.743	0.3021E 01	0.6085E 02	−0.7499E 02	−0.1414E 02	0.1245E 04
12.227	0.3062E 01	0.5071E 02	−0.7156E 02	−0.2085E 02	0.1076E 04
12.723	0.3103E 01	0.4118E 02	−0.6809E 02	−0.2691E 02	0.9677E 03
13.233	0.3144E 01	0.3194E 02	−0.6464E 02	−0.3270E 02	0.9355E 03
13.756	0.3185E 01	0.2242E 02	−0.6124E 02	−0.3882E 02	0.1050E 04
14.293	0.3226E 01	0.1047E 02	−0.5794E 02	−0.4747E 02	0.1990E 04

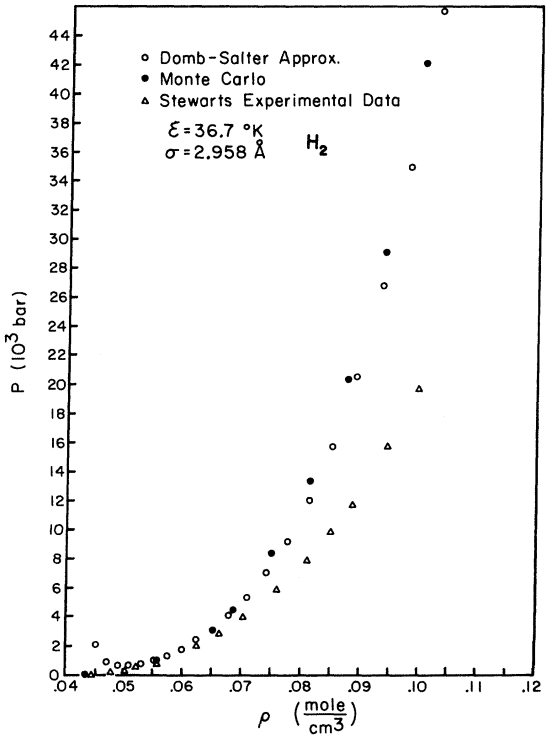

FIG. 1. Comparison of two theoretical state equations based on the Lennard-Jones potential with Stewart's data for H_2 ($T=0\,°K$).

In the case of H_2 for densities corresponding to pressures above 10^4 bar, this ratio is roughly 10% or less, which also suggests the validity of the usual Taylor-series expansion of the potential for these densities.

The equation of state for H_2 in the Domb-Salter approximation for a Lennard-Jones potential and from Ref. 2 is compared to experimental data[12] in Fig. 1. A comparison based on the Buckingham potential for H_2 of the equation of state calculated in the Domb-Salter approximation and by cluster-expansion methods[3] is shown in Fig. 6. Again the results of the two methods agree closely for pressures above 2000 bar. The calculated equations of state for the two potentials agree closely, but both give pressures larger than the experimental values; at the highest measured pressure this discrepancy is over 50%. The equation of state at $T=0\,°K$ calculated from Eq. (5.1) for D_2 (Fig. 7) shows a similar discrepancy with the experimental data of Ref. 12.

For He^3 and He^4 the energies given by the Domb-Salter approximation and by Monte Carlo agree closely for pressures above 20 000 bar. It is expected that for solid helium one must go to higher pressures than for hydrogen before the classical behavior is found, due to the weaker binding and

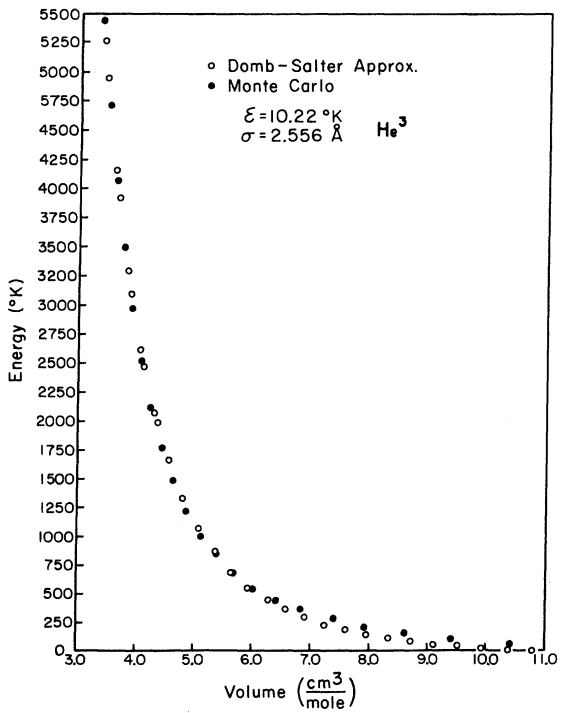

FIG. 2. Comparison of theoretical energy-vs-volume curves based on the Lennard-Jones potential for He^3 at $T=0\,°K$.

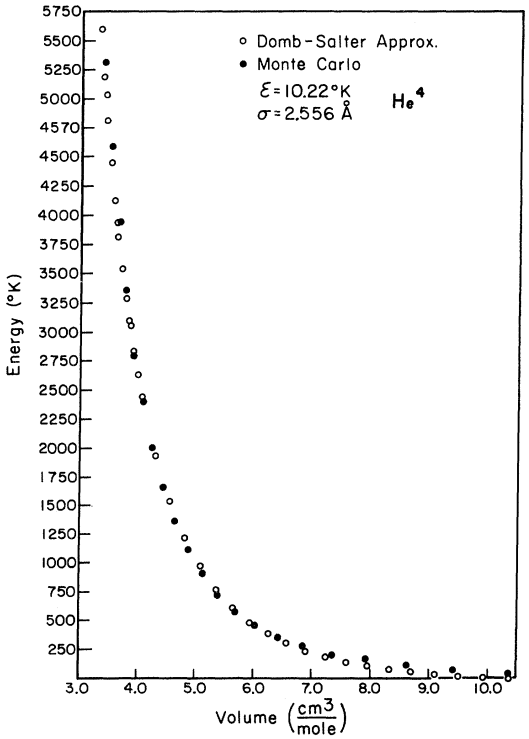

FIG. 3. Comparison of theoretical energy-vs-volume curves based on the Lennard-Jones potential for He^4 at $T=0\,°K$.

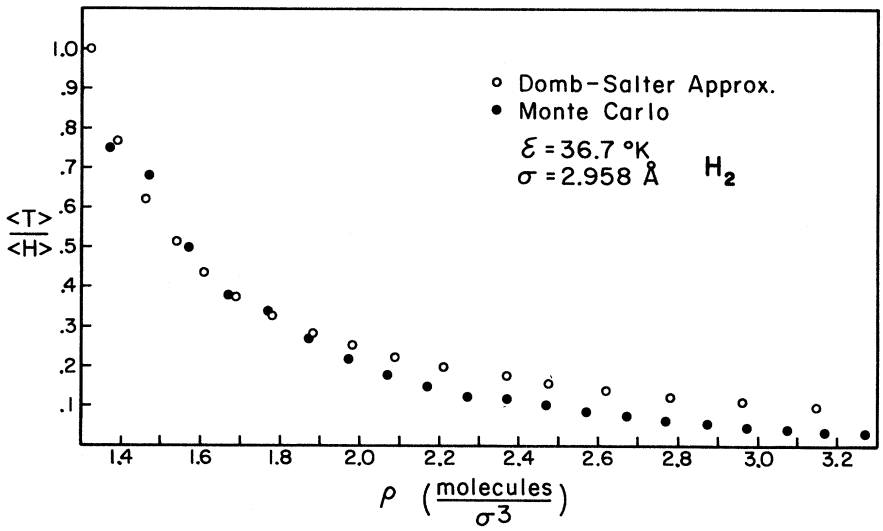

FIG. 4. Ratio of kinetic to total energy for H_2 based on the Lennard-Jones potential ($T = 0\,°K$).

thus increased anharmonicity of He. As expected on the basis of the masses the He^3 pressure is higher than that of He^4 at the same volume (Fig. 8). At a molar volume of 6.5 ml the zero-point energy (in the Domb-Salter approximation) and the static potential energy are nearly equal and the He^3

TABLE VI. Domb-Salter approximation for He^4 (Lennard-Jones potential).

Nearest-neighbor distance (Å)	Molar volume (ml)	Zero-point energy (°K)	Static potential energy (°K)	Total energy (°K)	Pressure (bar)
0.1958E 01	3.196	0.1835E 04	0.4614E 04	0.6449E 04	0.6704E 06
0.1999E 01	3.401	0.1583E 04	0.3450E 04	0.5032E 04	0.4933E 06
0.2040E 01	3.614	0.1368E 04	0.2574E 04	0.3943E 04	0.3653E 06
0.2081E 01	3.835	0.1186E 04	0.1915E 04	0.3100E 04	0.2721E 06
0.2121E 01	4.066	0.1030E 04	0.1416E 04	0.2446E 04	0.2038E 06
0.2162E 01	4.306	0.8962E 03	0.1039E 04	0.1935E 04	0.1535E 06
0.2203E 01	4.555	0.7815E 03	0.7533E 03	0.1535E 04	0.1162E 06
0.2244E 01	4.813	0.6827E 03	0.5367E 03	0.1219E 04	0.8839E 05
0.2285E 01	5.081	0.5973E 03	0.3727E 03	0.9700E 03	0.6754E 05
0.2326E 01	5.359	0.5234E 03	0.2487E 03	0.7721E 03	0.5184E 05
0.2367E 01	5.646	0.4592E 03	0.1552E 03	0.6145E 03	0.3995E 05
0.2408E 01	5.944	0.4033E 03	0.8510E 02	0.4884E 03	0.3091E 05
0.2449E 01	6.252	0.3546E 03	0.3279E 02	0.3874E 03	0.2400E 05
0.2490E 01	6.571	0.3120E 03	−0.5855E 01	0.3061E 03	0.1870E 05
0.2530E 01	6.900	0.2746E 03	−0.3404E 02	0.2406E 03	0.1462E 05
0.2571E 01	7.240	0.2418E 02	−0.5422E 02	0.1876E 03	0.1147E 05
0.2612E 01	7.591	0.2129E 03	−0.6829E 02	0.1446E 03	0.9017E 04
0.2653E 01	7.953	0.1874E 03	−0.7770E 02	0.1097E 03	0.7111E 04
0.2694E 01	8.327	0.1648E 03	−0.8356E 03	0.8126E 02	0.5622E 04
0.2735E 01	8.712	0.1448E 03	−0.8676E 02	0.5806E 02	0.4457E 04
0.2776E 01	9.108	0.1270E 03	−0.8795E 02	0.3908E 02	0.3543E 04
0.2817E 01	9.517	0.1112E 03	−0.8765E 02	0.2352E 02	0.2826E 04
0.2858E 01	9.937	0.9698E 02	−0.8626E 02	0.1072E 02	0.2262E 04
0.2899E 01	10.370	0.8425E 02	−0.8409E 02	0.1535E 00	0.1820E 04
0.2939E 01	10.815	0.7276E 02	−0.8138E 02	−0.8616E 01	0.1474E 04
0.2980E 01	11.273	0.6234E 02	−0.7830E 02	−0.1595E 02	0.1206E 04
0.3021E 01	11.743	0.5282E 02	−0.7499E 02	−0.2217E 02	0.1003E 04
0.3062E 01	12.227	0.4402E 02	−0.7156E 02	−0.2754E 02	0.8561E 03
0.3103E 01	12.723	0.3574E 02	−0.6809E 02	−0.3235E 02	0.7642E 03
0.3144E 01	11.233	0.2773E 02	−0.6464E 02	−0.3691E 02	0.7391E 03
0.3185E 01	13.756	0.1946E 02	−0.6124E 02	−0.4178E 02	0.8419E 03
0.3226E 01	14.293	0.9086E 01	−0.5794E 02	−0.4885E 02	0.1662E 04

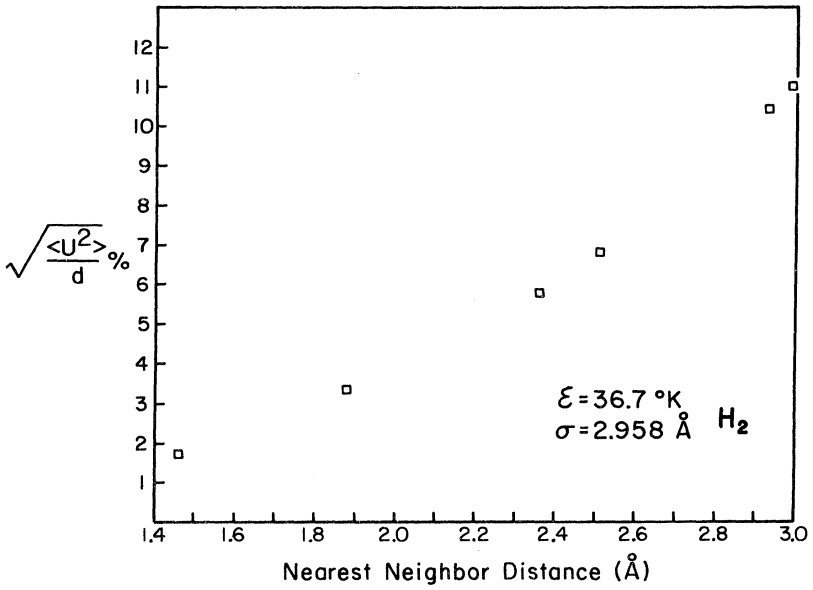

FIG. 5. Ratio of RMS displacement to nearest-neighbor distance. Calculated in harmonic approximation for H_2 with Lennard-Jones potential ($T=0$ °K).

pressure is roughly 10% larger than the He^4 pressure. As the molar volume decreases the static potential energy dominates and the He^3 and He^4 pressures converge, differing by about 3% at 2×10^5 bar. Experimental data of Dugdale and Simon,[13] Dugdale and Franck,[14] and of Stewart are also given for comparison in Fig. 8. Stewart's data was taken at 4 °K; however, values of the thermal-expansion coefficient and compressibility for molar volumes above 10.5 ml in Dugdale and Simon show the correction to the pressure at $T=0$ °K as quite undetectable on the scale on Fig. 8 in this region.

In the case of Ne^{20} (Fig. 9), the pressure from Eq. (5.1) is compared with results of a Monte Carlo calculation[15] where both use a Lennard-Jones potential[16] with $\sigma=2.786$ Å and $\epsilon=36.76$ °K. Agreement is essentially exact within the fluctuations of the Monte Carlo results. The experimental results have a similar form with a shift in the molar volume scale of roughly 0.5 cm^3. Although no sys-

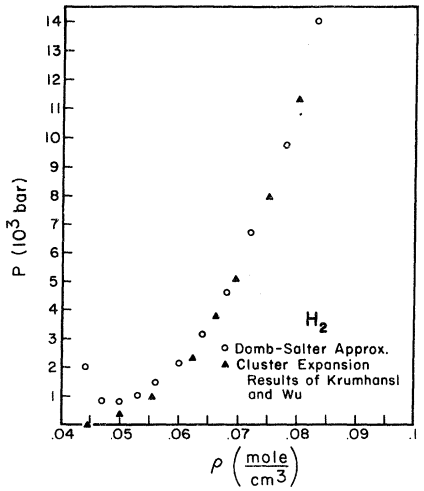

FIG. 6. Comparison of the equation of state for a Buckingham potential calculated in the Domb-Salter approximation and by cluster expansion for H_2 ($T=0$ °K).

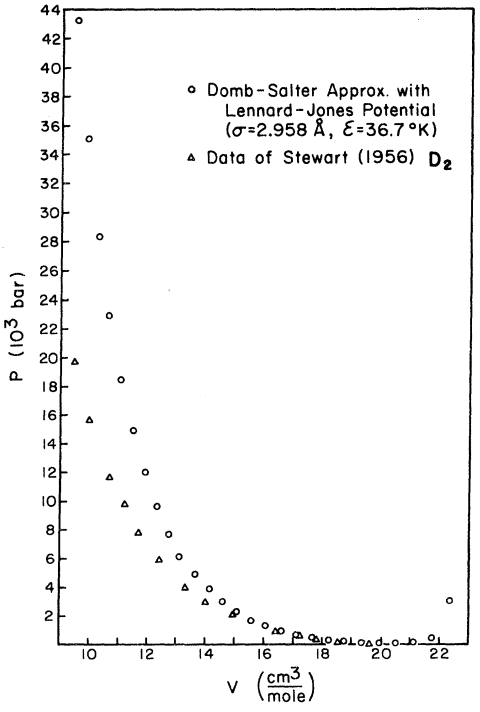

FIG. 7. Equation of state for D_2 at $T=0$ °K.

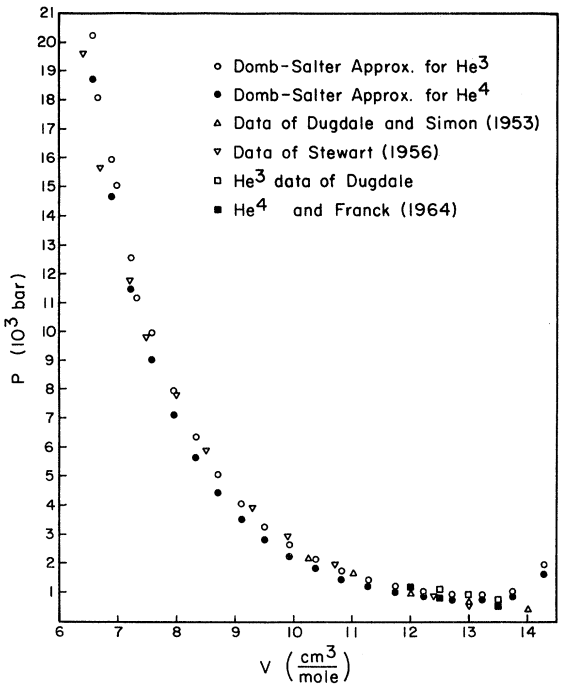

FIG. 8. Equation of state for He^3 and He^4 at $T=0\,°K$.

tematic attempt to find parameters to fit the experimental results was made, we also show pressures calculated from 5.1 for a slightly larger value of σ.

In the Domb-Salter approximation for pressures above 10^3 bar, the nearest-neighbor distance in terms of σ units (the Lennard-Jones distance parameter) is less for He than for H_2. This is because of the large compressibility of He and means that for pressures above 10^3 bar a potential accurate at small distances will be as much or more important to a correct calculation of the state equation of He than is the case for H_2. Noting this and in view of the substantial agreement between theory and experiment for He, the discrepancies between theory and experiment for H_2 (Fig. 1) may not be due solely to the inadequacy of a Lennard-Jones potential in representing the core region. The agreement between the calculated state equations for H_2 based on the Lennard-Jones and Buckingham potential further suggests that additional experimental data for H_2 at even moderately high pressures would be useful.

VII. SUMMARY

In this paper several criteria for the validity of the harmonic approximation at high density have been given: (i) decreasing ratio of rms displacement to nearest-neighbor distance; (ii) decreasing ratio of zero-point to total energy; (iii) comparison with experiment and Monte Carlo calculations.

The density at which the harmonic approximation should be accurate varies according to which criterion is applied with (iii) giving the lowest density. Lastly using results of Maradudin and Flinn[17,18] for a nearest-neighbor-model fcc crystal, it is possible to estimate the contribution to the energy and pressure of the lowest-order cubic and quartic terms in the conventional perturbation expansion. These terms give significant (10% or more) corrections to the harmonic state equations of D_2, H_2, He^3, and He^4 below 5×10^3 bar and to the ground-state energies of H_2, D_2, and He^3, He^4 below 7×10^4 and 15×10^4 bar, respectively. The present agreement with experiment and Monte Carlo calculations below these pressures would not be maintained if these corrections were added. In view of this it may be conjectured that an exact rather than lowest-order perturbation theoretic calculation would restore this agreement and show the harmonic approximation to be accurate, as suggested by criterion (iii), at densities only slightly above those where instability is indicated. We stress that this is conjecture. The calculations presented show that in the worst case a harmonic model would be adequate for the solids considered at pressures well below those of interest in astrophysical calculations or molecular solid to metallic phase transitions.

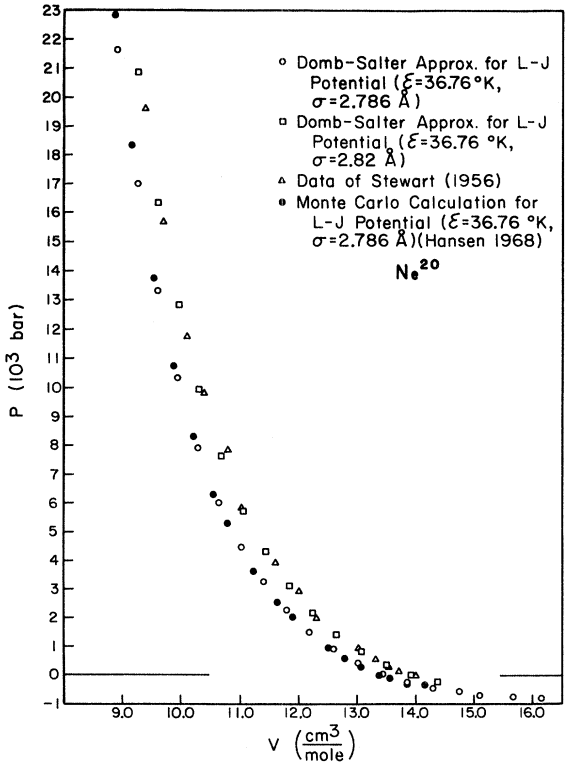

FIG. 9. Equation of state for Ne^{20} at $T=0\,°K$.

Lastly we comment on the implication of these calculations for various quantum crystal calculations. While it is perfectly clear that at low pressure (see Figs. 1, 6 and 8) the classical method breaks down, and that quantum crystal methods are necessary, it is also apparent that at high density the atom motion is dominated by the single site potential rather than by short-range correlation effects. Our results, together with those of Chell,[19] lead us to differ with Horner[20]; we conclude that short-range correlations at high density may be adequately accounted for in the harmonic approximation.

ACKNOWLEDGMENTS

We wish to thank various of our colleagues for their comments, and also Dr. M. L. Klein who points out that though the method used in this paper has frequently given a reasonable volume dependence of the free energy, it is not so dependable for strain-dependent quantities.[21]

---

†Work supported by the U. S. Atomic Energy Commission under contract No. AT(30-1)-3699, Technical Report No. NYO-3699-51.

[1]C. Domb and L. Salter, Phil. Mag. 43, 1083 (1952).

[2]T. A. Bruce, preceding paper, Phys. Rev. B 5, 4170 (1972).

[3]S. Y. Wu, Materials Science Center, Cornell University, MSC Report No. 783, 1967 (unpublished).

[4]J. P. Hansen and D. Levesque, Phys. Rev. 165, 293 (1968).

[5]A. A. Maradudin, E. W. Montroll, and G. H. Weiss, *Theory of Lattice Dynamics in the Harmonic Approximation* (Academic, New York, 1963).

[6]D. C. Wallace and J. L. Patrick, Phys. Rev. 137, A152 (1965).

[7]C. Isenberg, Phys. Rev. 132, 2427 (1963).

[8]Reference 4, p. 240, Eq. (7.2.22).

[9]A. M. Michels, W. de Graaft, and C. A. ten Seldam, Physica 26, 393 (1960).

[10]J. de Boer and A. Michiels, Physica 5, 945 (1938).

[11]I. B. Srivastava and A. K. Barua, Indian J. Phys. 35, 320 (1961).

[12]J. W. Stewart, J. Phys. Chem Solids 1, 146 (1956).

[13]J. S. Dugdale and F. E. Simon, Proc. Roy. Soc. (London) A257, 291 (1953).

[14]J. S. Dugdale and J. P. Franck, Phil. Trans. Roy. Soc. London, Ser. A 257, 1 (1964).

[15]J. P. Hansen, Phys. Rev. 172, 3 (1968); 172, 919 (1968).

[16]J. S. Brown, Proc. Phys. Soc. (London) 89, 987 (1966).

[17]A. A. Maradudin and P. A. Flinn, Ann. Phys. (N. Y.) 22, 223 (1963).

[18]J. L. Feldman and G. K. Horton, Proc. Phys. Soc. (London) 92, 227 (1967).

[19]G. G. Chell, J. Phys. C 3, 1861 (1970).

[20]H. Horner, Solid State Commun. 9, 79 (1971).

[21]T. H. K. Barron and M. L. Klein, Proc. Phys. Soc. (London) 82, 161 (1963).